Toward a simple physical model of double-reed musical instruments: influence of aero-dynamical losses in the embouchure on the coupling between the reed and the bore of the resonator.

C. Vergez[1], A. Almeida[2], R. Caussé[2] and X. Rodet[2]

[1] LMA, CNRS, 31 Chemin Joseph Aiguier, 13402 Marseille Cedex 20

[2] IRCAM, CNRS/Centre G. Pompidou, 1. Pl. Igor Stravinsky, 75004 Paris

Abstract

The air flow model usually considered for physical modeling of wind instruments has to be modified for double-reed instruments. Indeed, it is usually assumed in simple models that air pressure in the reed channel is the same as air pressure at the input of the bore. On the contrary, the first aim of this paper is to explain that, because of geometrical specificities of the embouchure of double-reed instruments, this assumption can hardly be applied to double reed modeling. A refined (yet still quasi-stationary) model is then proposed, where air pressure at the inlet of a double reed channel and at the input of the bore are linked by a nonlinear relation. This relation is parameterized by a single coefficient which captures all the differences with the usual flow model, and reduces to the simple model when this coefficient is zero. This allows an analytical comparison between both models. The second aim of the paper is to study the influence of the flow model on the auto-oscillation of the well known Backus model of reed instruments. Three possible behaviors, qualitatively different, are identified according to the magnitude of the nonlinear term characterizing the double reed flow model. Two of these behaviors may present an hysteretic character. Analytical predictions are in agreement with numerical simulations.

1 Introduction

Wind musical instruments have similar principles of functioning: the player, by blowing inside the instrument destabilizes a valve (a simple reed, a double reed or two lips). The acoustic response of the instrument acts as a feedback loop which influences the valve behavior. The production of a sound corresponds to the auto-oscillation of this dynamical system. Obviously, in spite of these similarities, the functioning of each class of instruments possesses its own specificities.

Our aim is to identify one or several specificities for each class of instruments in order to propose physical models (simple, therefore possibly caricatural). We are currently interested in characterizing the class of double reed instruments (oboe, bassoon, bagpipes ...) in particular compared to simple reed instruments (like the clarinet).

The most obvious difference is, as suggested by names, the number of reeds. However, both parts of a double reed are the same and stroboscopic visualisations of oboe reed oscillations reveal symetric displacements for usual playing conditions (see figure 1 for an illustration when the

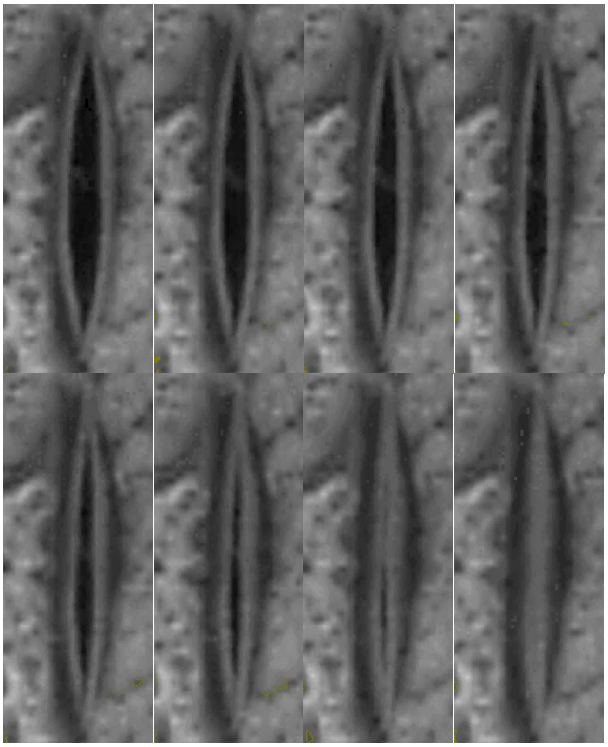

Figure 1: Stroboscopic visualisations of an oboe double-reed corresponding to the closure phase and showing symetric displacements of both sides of the reed. The oboe is blown through an artificial mouth.

oboe is blown through an artificial mouth[1]). This justifies the choice of a single-mode model, like for a simple reed.

A second major difference between the clarinet and the oboe is the inner shape of the resonator, which is nearly cylindrical for the clarinet and nearly conical for the oboe. Input impedances are therefore very different, but this is not a discriminating factor between simple reed and double reed instruments : indeed, a simple reed exciting a conical bore is not a oboe, but a saxophone ! Moreover, it is possible to find examples of instrument made up by a double reed and a cylindrical bore (for instance the crumhorn, a Renaissance instrument).

A third difference is linked to the geometry of the embouchure : its cross section is large compared to the cross section of the reed channel for the clarinet or the saxophone, whereas these cross sections are of the same order of magnitude for most double-reed instruments (see figures 3 and 4). This geometrical difference does not allow the same hypothesis to be applied as far as air flow modeling inside the reed channel is concerned. Indeed, former studies suggest that a pressure with a non-zero mean value stands inside a double reed ([2]). Within the scope of a non lumped model this pressure decreases along the backbore of the double-reed because of visco-thermal and/or turbulent losses ([3]).

This work is focussed on this particular aspect of the physics of reed-instruments: the influence of the embouchure geometry on the modeling of the air flow and its influence on the auto-oscillation of the global model.

Problem statement is detailed in section 2. Compared to the classical model used for clarinet (see [4] or [5], summarized in section 3) a quasi-stationary flow model in oboe is described in section 4. Differences between the two flow models may be reduced to an additional aerodynamical nonlinearity in the case of the oboe. Its influence on the auto-oscillation of the model is studied in section 5, where analytical predictions are also compared to numerical simulations.

2 Problem Statement

2.1 Woodwinds general functioning

For readers unfamiliar with woodwind instruments, the general functioning of these instruments is recalled in this section, and the name of the variables involved in the modeling of each of these parts (and used further in the core of the paper) is precised (see figure 2 for a summary). Four parts can be distinguished.

The mouth: where the static pressure p_m imposed by the player, creates an air flow through the instrument (p_m is thereby called the blowing pressure, and is considered as a given parameter in the following).

[1] see [1] for details

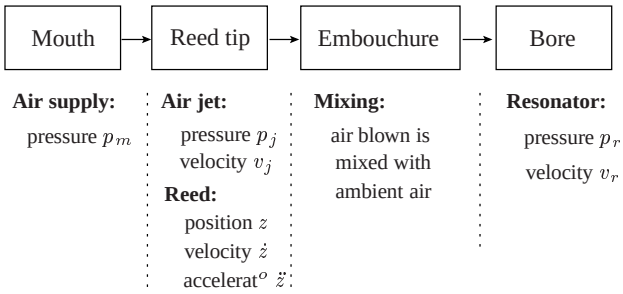

Figure 2: Scheme showing the main parts of a woodwind instrument and the name of the variables associated to them in this paper.

The reed tip dynamics: (represented by the reed position z on the vertical axis, and its successive time derivatives $\dot{z}$ and $\ddot{z}$) responsible for a change in the cross section through which the air flows, and so responsible for the volume flow q entering the embouchure for a given velocity v_j. This volume flow q can be calculated from the equation governing the reed motion, where the blowing pressure p_m and the air pressure just under the reed tip p_j appear (see section 3).

The embouchure: where the air blown is mixed with ambient air. Therefore the air pressure and velocity at the inlet of the reed channel (p_j and v_j) are "transformed" through the embouchure into p_r and v_r, at the input of the resonator. Note that p_j, v_j, p_r and v_r are unknown and have to be calculated.

The resonator: responsible for the relationship between p_r and v_r expressed by a convolution equation where the impulse response of the resonator $g(t)$ appears ($g(t)$ is considered to be known in this study).

The simulation of the whole instrument can be done by solving simultaneously all the equations representing the aforementioned four parts (mouth, reed tip, embouchure, bore), as shown in section 3.

2.2 Focus of the paper

As explained in the introduction, this paper focuses on the influence of the embouchure geometry on the modeling of the air flow.

In the case of clarinet-like instruments, it is widely accepted ([6]) that the flow through the embouchure can be described by (see section 3 for details):

$$\begin{cases} p_m &= p_j + \frac{1}{2}\rho v_j^2 \\ p_j &= p_r \end{cases} \tag{1}$$

It is first shown in section 4, how geometrical specificities of oboe-like embouchures can lead to a different (yet simple) model for the flow:

$$\begin{cases} p_m &= p_j + \frac{1}{2}\rho v_j^2 \\ p_j &= p_r + \frac{1}{2}\rho\Psi\frac{q^2}{S_{ra}^2} \end{cases} \tag{2}$$

where Ψ can be considered constant under certain assumptions and appears to stand for different losses mechanisms in the embouchure.

Then in section 5, both flow models are coupled to a basic model of the reed dynamics and of a cylindrical resonator. Results are compared, from an analytical and a numerical point of view, when varying parameter Ψ ($\Psi = 0$ in equation (2) being equivalent to equation (1)).

It is therefore important to note that we are not concerned in this paper by other important aspects of the modeling. For example only a simple model for the reed will be considered, without taking into account the presence of the lips (case of the oboe or of the basson) or not (case of the crumhorn or the bagpipes). Indeed, at this stage of the study, our aim is not to propose a complete model of an existing instrument, with comparisons between experimental and simulation results. This explains why this work is mainly analytical or numerical. Moreover, the willing to compare results with the well known model of clarinet-like instruments also explains why only cylindrical bores are considered in the following.

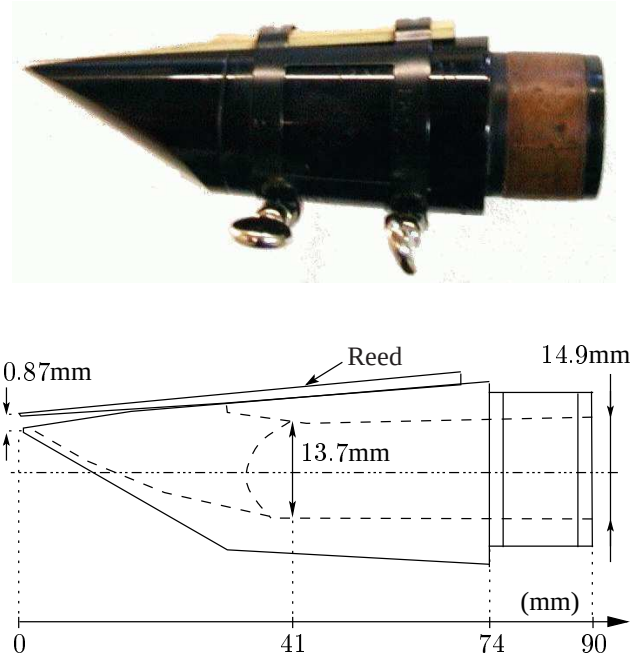

Figure 3: Embouchure of a clarinet (upper part) and its longitudinal cut (lower part).

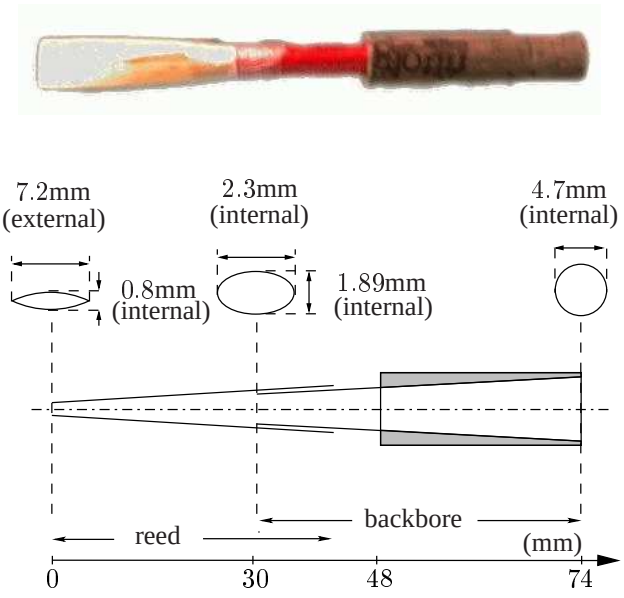

Figure 4: Embouchure of an oboe (upper part) and its longitudinal cut (lower part). Measurements have been done by A. Terrier (mechanic at IRCAM)

3 Classical model of a single-reed instrument

In this section, basic principles of the clarinet functioning are briefly recalled. Simple models have been proposed by [4], [7], [8], [9], or [10] for example of pioneers. The reed is often modelled as a mass/spring/damper oscillator. However, because of a resonance frequency ($\simeq$ 3000Hz) large compared to the first harmonics of typical playing frequencies, inertia and damping are often neglected ([7]). This hypothesis leads, considering that reed dynamics is governed by the pressure difference accross the reed to :

$$k_s(z - z_0) = (p_j - p_m) \tag{3}$$

where z (z_0) is the reed position (at rest)[2], k_s is the reed surfacic stiffness, p_m and p_j are the pressure deviation in the mouth and under the reed tip respectively.

As noted by Hirschberg in [11], in the case of clarinet-like instruments, the control of the volume flow by the reed position is due to the existence of a turbulent jet. Indeed, a jet is supposed to form in the embouchure (pressure p_j) after the flow separation from the walls, at the end of the (very short) reed channel (see figure 3). Neglecting the velocity of air flow in the mouth compared to jet velocity v_j, The Bernoulli theorem applied between the mouth and the reed channel leads to:

$$p_m = p_j + \frac{1}{2}\rho v_j^2 \qquad \text{with } q = \alpha S_i v_j \tag{4}$$

where S_i is the cross section at the inlet. Since this area can be expressed as the product between the reed opening z and the reed width w_r (not visible in figure 3 since it is transversal to the plane of the figure), equation (4) can be re-written as follows:

$$q = \alpha z w_r \sqrt{\frac{2}{\rho}(p_m - p_j)} \tag{5}$$

where q is the volume flow accross the reed, w_r is the width of the reed and ρ is the air density. Parameter α is semi-empirical and stands for jet contraction at the beginning of the reed channel (*vena contracta* effect). Through

[2] Thus the reed is closed when $z = 0$ and opened when $z > 0$

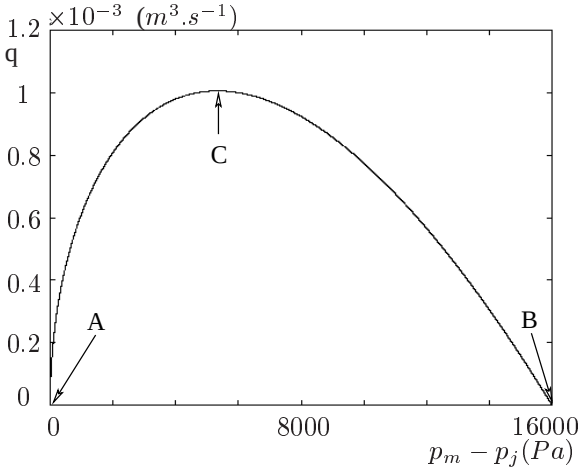

Figure 5: Volume flow calculated according to equation (6) with $\alpha = 1$, $z_0 = 1e^{-3}$m, $w_r = 1.6e^{-2}$m, $k_s = 1.6e^{7}$Pa.m^{-1} and $p_m = 8e^{3}$Pa.

papers already published, it can be found that α varies between $\alpha = 0.61$ and $\alpha = 1$, i.e. no vena-contracta (see for example Wilson and Beavers ([9]) or Gilbert [12]). This difference seems mainly due to the high dependence of the structure of the flow on the Reynolds number.

Combining equations (3) and (5) leads to the well-known expression of the volume flow as a function of the pressure difference across the reed (graphical sketch in figure 5):

$$q = \alpha w_r (z_0 - \frac{1}{k_s}(p_m - p_j))\sqrt{\frac{2}{\rho}(p_m - p_j)} \qquad (6)$$

According to equation (6), it is obvious that the volume flow is 0 either when $p_m = p_j$ (point A in figure 5) or when $p_m - p_j = z_0 k_s$ (point B in figure 5). Note that for $(p_m - p_j) \geq z_0 k_s$, the reed is closed. Another remarkable point, noted C in figure 5, corresponds to the maximum volume flow through the instrument. This maximum is reached when $p_m - p_j = \frac{1}{3} z_0 k_s$.

Since the cross section of the embouchure is large compared to the cross section of the reed channel, it can be supposed that all the kinetic energy of the jet is dissipated through turbulence with no pressure recovery (like in the case of a free jet). Therefore, the pressure in the jet is (assuming pressure continuity) the acoustic pressure p_r imposed by the resonator response to the incoming volume flow q (within the hypothesis of linear acoustics) :

$$p_j = p_r = g * q \qquad (7)$$

where g is the impulse response of the resonator.

4 Simple model of the air flow in a double reed

4.1 Specificities of double reeds

The specific geometry of the double reed of an oboe (for example[3]) calls the relevance of the flow model presented in section 3 in question. Indeed in this model, the control of the volume flow by the reed is ensured by the turbulent mixing in the embouchure. This supposes, on the one hand the formation of a jet, and on the other hand the turbulent dissipation of its kinetic energy in the embouchure. Let us evaluate the validity of these hypothesis in the case of oboe-like instruments, in the light of two geometric considerations.

4.1.1 Low conicity of the reed channel

According to the dimensions of a clarinet embouchure (see figure 3), the separation of the flow from the walls is likely to occur at the end of the reed channel (great and rapid increase of the cross section). On the contrary in the embouchure of an oboe (see figure 4), the cross section increases slightly and continuously, the inner profile being close to a slowly diverging cone. However a jet is expected to form at the inlet of the reed channel, more especially since the thickness of the reed is small compared to the opening (in fact its mean value averaged in time, noted d) and because of a Reynolds num-

[3]For sake of simplicity, “clarinet” and “oboe” are used instead of “single-reed instruments” or “double-reed instruments”

ber (adimensioned by d) quite large ($Re_d = \frac{Vd}{\nu} \simeq 1700$ with $\nu = 1.8e^{-5}$kg.m^{-1}.s^{-1}, $d = 8e^{-4}$m and $V = \sqrt{2p_m/\rho} \simeq 39$m.s^{-1} if $p_m = 1e^3$Pa).

4.1.2 Confinement of the jet

Assuming that a jet has formed at the inlet of the reed-channel, the free jet dissipation model seems hardly applicable. Indeed, the cross section of the jet is not negligible compared to the cross section of the reed.

4.2 Incompressible quasi-stationary model

As long as experimental observations of the velocity field inside the flow are not available (PIV experiments are currently being prepared) we can only speculate on what occurs in a double reed. It is however possible to make assumptions inspired by geometrical considerations, estimation of dimensionless characteristic numbers, existence of analytical solutions for simpler cases, or simulation results already published.

The Mach number $Ma = V/c$ being of the order of 10^{-1}, air compressibility is neglected in the reed. Moreover a quasi-stationary model is considered. It is worth noting that the Strouhal number St_{Lr} adimensionned by the length of the reed is of the order of 10^{-2} for simple reed instruments ([13]). However in the case of the oboe $St_{L_r} = \frac{fL_r}{v_j}$ is of the order of 10^{-1} for a frequency $f = 440Hz$, a reed length $L_r = 26mm$ and a blowing pressure $p_m = 1e^4Pa$. Therefore, the following model has to be considered carefully, particularly for low blowing pressures and/or high frequencies.

4.2.1 Inlet of the reed channel : jet formation

The oboe player grips the reed between his/her lips at a few millimeters from its extremity. A small part of the reed is therefore inserted in the mouth without any contact with the lips. Thus, the problem resembles to the case of a tube re-enterring inside a cavity (the mouth). Then, it can be supposed that for a high enough Reynolds number, there is formation of a jet at the input. Moreover the limit case of the Borda tube where viscosity can be neglected (infinite Re_d) is well known and within the frameworks of potential theory ([14], p27-43) it is demonstrated that a jet with a cross section being half of the cross section at the input S_i is formed ($\alpha = \frac{S_j}{S_i} = 1/2$). Therefore, it seems reasonable to assume the formation of a jet at inlet of the double-reed channel, with cross-section αS_i. This assumption seems commonly supported in the literature ([6]). The pressure and the velocity of the jet, respectively p_j and v_j, and the volume flow q are linked by:

$$p_m = p_j + \frac{1}{2}\rho v_j^2 \qquad \text{with} \qquad q = \alpha S_i v_j \tag{8}$$

The air velocity in the mouth is neglected like in the clarinet model (equation (8) is in fact the same as equation (4)).

Experiments carried out by Gokhshtein [15] show that rounding the edges of a bassoon double reed reduces significantly the inlet losses due to flow separation from the sides of the reeds. This would correspond in the model to having α closer to 1, since $\alpha = 1$ means no separation at the reed inlet. However, as it is pinpointed in Gokhshtein paper, the shape of reeds sold to musicians has not been controlled to date: “they are squared off at the tip”.

4.2.2 Jet re-attachement and/or turbulence

Once the jet has formed, taking into account air viscosity leads to two possible scenarii.

First possibility, the flow reattaches to the wall (see figure 6): because of momentum diffusion due to air viscosity, air around the jet is accelerated. This creates a low pressure area which tends to attract the jet to the walls. After a certain length, re-attachement occurs. Numerical simulations at different Re_d and for different openings

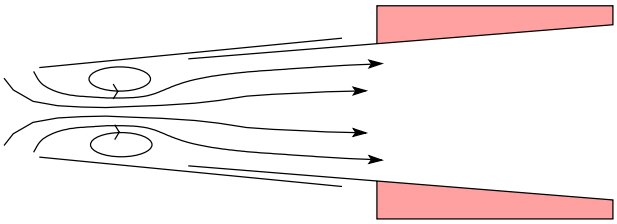

Figure 6: After the jet formation at the entry of the double reed, the flow may reattach to the walls. Streamlines are shown.

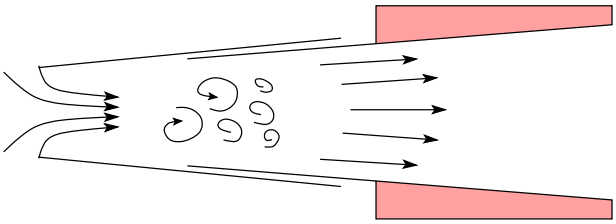

Figure 7: After the jet formation at the entry of the double reed, turbulent mixing may occur.

by Hirschberg and colleagues ([13], within the hypothesis of an incompressible, stationary non turbulent fluid) show that this behavior is typical, and includes a vortex in the area where the flow is separated from the walls.

Second possibility, the jet structure is destroyed by turbulence (see figure 7): in this case, because of geometrical considerations already mentioned, the kinetic energy dissipation is only partial. After a mixing region, the flow is spread over the whole cross section.

Macroscopic Modelling: even if in both cases (reattachement or turbulence) the precise description of the flow dynamics is out of purpose, a macroscopic model can be used to describe the discharge losses Δe_{tr} caused by vortices or turbulence. Indeed, a theoretical estimation given by the mass conservation, and the momentum conservation is ([16], p199):

$$\Delta e_{tr} = \frac{1}{2}\rho v_j^2 \left(1 - \frac{S_j}{S_{ra}}\right)^2 \qquad (9)$$

where v_j is the jet velocity, S_j is the cross section of the jet, and S_{ra} is the cross section of the reed at the place where the flow is spread over the whole cross section (possibly after jet re-attachement).

Equation (9) is a crude model but behaves reasonably well in limit cases. Indeed, when $S_j = S_{ra}$ (i.e. no jet formation), equation (9) reduces to $\Delta e_{tr} = 0$, as expected. Moreover, when $S_j/S_{ra} \to 0$ (case of the clarinet), $\Delta e_{tr} \to \frac{1}{2}\rho v_j^2$, i.e. all the kinetic energy of the jet is dissipated through turbulent mixing. Therefore, equation (9) is used in the following as a simple way of taking into account effects of re-attachement and/or turbulent mixing.

4.2.3 The flow downstream in the reed (including the backbore)

Whatever the solution considered (re-attachement or turbulent mixing), a flow spread over the full cross-section of the reed takes place after a certain distance. Then one can consider that other falls of pressure take place downstream, in the late part of the reed. Two main phenomena can be responsible of these falls of pressure.

Visco-thermal losses due to wall interaction: visco-thermal losses are all the more significant as the cross section area is smaller. However, as seen in section 4.2.1, the flow is supposed to be separated from the walls in the narrowest part of the reed channel, close to the inlet, where the geometry is essentially bidimensional. Then interaction with the wall is only considered downstream in the reed, where the reed becomes closer to a cone.

Visco-thermal losses can be modelled by unit discharge losses. Discharge losses Δe_f in a cylindrical pipe (the low conicity of the reed channel is neglected in this approximation) with diameter d, length L_r, and a flow with velocity v_c can be written ([17], p177):

$$\Delta e_f = \frac{1}{2}\rho \frac{L_r}{d} \zeta_f v_c^2 \qquad (10)$$

In equation (10), ζ_f is the unit discharge loss coefficient. It

can be evaluated using the Nikuradse diagram ([17], p217) according to the wall roughness ϵ, to the diameter d and to the Reynolds number. However, to the authors knowledge, the wall roughness of cane reeds has never been studied experimentally. Therefore, choosing a value for ϵ is a difficult task. On the other hand, for laminar flows, ζ_f is known analytically (Poiseuille flow):

$$\zeta_f = \frac{64}{Re_d} \tag{11}$$

It is generally admitted that equation (11) can be used in cylindrical pipe for $Re_d < 2000$.

Singular discharge losses due (for example) to a new separation of the flow, which can occur further downstream, more particularly if there is a narrowing of the cross-section like in some ancient double reed instruments ([6]). However, in an oboe or a bassoon, one does not observe such a narrowing. Separation can also be caused by the widening of the cross section. Note that practically, a new flow separation is generally not expexted in a conical pipe with an opening angle being less than 7 degrees ([17] p 143), which is the case in the oboe or the bassoon. However, singular discharge losses due to the conical widening can be estimated using a semi-empirical model proposed by Ouziaux and Perrier ([17], p143) for conical diffusers :

$$\Delta e_{diff} = \frac{1}{2}\rho v_{c_1}^2 \left(1 - \frac{S_{c_1}}{S_{c_2}}\right)^2 \sin\beta \tag{12}$$

where S_{c_1} and S_{c_2} are the cross section at the input and at the output of the conical diffuser, v_{c_1} is the velocity of the flow through section S_{c_1}, and β is the opening angle of the cone. Singular losses due to the widening of double reeds are expected to be low for moderate Re_d, which is predicted by equation (12) for small β and S_{c_1}/S_{c_2} close to 1.

4.3 Energy balance

Additivity of discharge losses is assumed (which is only an approximation, cf. [17], p231), and energy conservation is written between the mouth (pressure p_m, velocity neglected) and the entry of the resonator (pressure p_r, velocity v_r) (cf. [17] p179) where the flow is supposed to meet no resistance:

$$p_m = p_r + \frac{1}{2}\rho v_r^2 + \Delta e_{tr} + \Delta e_{diff} + \Delta e_f \tag{13}$$

Note that equation (13) is a commonly used modified version of the Bernoulli equation for steady incompressible flow. Using equations (9), (10) and (12) leads to:

$$\begin{aligned} p_m &= p_r + \frac{1}{2}\rho v_r^2 + \frac{1}{2}\rho v_j^2 \left(1 - \frac{S_j}{S_{ra}}\right)^2 \\ &\quad + \frac{1}{2}\rho v_{c_1}^2 \left(1 - \frac{S_{c_1}}{S_{c_2}}\right)^2 \sin\beta + \frac{1}{2}\rho \frac{L_r}{d}\zeta_f v_r^2 \end{aligned} \tag{14}$$

This equation can be rewritten in a more concise form:

$$\begin{cases} p_m = p_j + \frac{1}{2}\rho v_j^2 & (15a) \\ p_j = p_r + \frac{1}{2}\rho \Psi \frac{q^2}{S_{ra}^2} & (15b) \end{cases} \tag{15}$$

In equation (15), Ψ depends on the variables of the model:

$$\begin{aligned} \Psi &\triangleq \left(\frac{S_{ra}}{S_r}\right)^2 + \left(\frac{S_{ra}}{S_j}\right)^2 \left[-1 + \left(1 - \frac{S_j}{S_{ra}}\right)^2\right] \\ &\quad + \left(\frac{S_{ra}}{S_{c1}}\right)^2 \left(1 - \frac{S_{c1}}{S_{c2}}\right)^2 \sin\beta + \left(\frac{S_{ra}}{S_c}\right)^2 \frac{L_r}{d}\zeta_f \end{aligned} \tag{16}$$

In the case where the jet emerges in a large cavity (S_r and S_{ra} large, compared to S_j), equation (15) reduces to the classical model of a clarinet ($\Psi = 0$) after re-writting (15b) as a function of q^2/S_j^2 instead of q^2/S_{ra}^2.

4.4 Simplifying assumptions

In order to study in section 5, the influence of Ψ on the auto-oscillation of the system, we seek an approximate expression of Ψ constant. The part of the reed which oscillates (upstream from the contact area between the lips and the reed, in the thinest part of the reed) is supposed to have

a length of the same order of magnitude as the length of the reed where the flow is separated from the walls. This hypothesis allows us to write $S_{ra} \simeq S_{c1} \simeq S_c = const$ and $S_{c2} = S_r = const$. Therefore, in equation (16), the term $\frac{S_{ra}}{S_j}$ is the only one to depend on the opening of the reed. In order to study the auto-oscillation of the model, we get rid of this dependency, by using the mean value of S_j averaged in time $< S_j >_t$ instead of S_j (for example along a period when the model's asymptotic behavior is periodic). If we note $\Gamma = S_{c1}/S_{c2}$, equation (16) can then be rewritten:

$$\begin{aligned} \Psi &\simeq \Gamma^2 + \left(\frac{S_c}{<S_j>_t}\right)^2 \left[-1 + \left(1 - \frac{<S_j>_t}{S_c}\right)^2\right] \\ &+ (1-\Gamma)^2 \sin\beta + \frac{L_r}{d}\zeta_f \end{aligned} \tag{17}$$

In the following, Ψ is taken constant.

5 Influence of losses on the auto-oscillation of the model

In this section, the influence of Ψ on the auto-oscillation of the model is considered. More precisely, the model presented in section 3 (representative of the basic behavior of simple reed instruments) is compared to the model presented in section 4. For this latter model, equations (3), (5) and (6) are still valid but the jet pressure p_j is no more the acoustic pressure p_r. On the contrary, p_j and p_r are now linked by the second equation of system (15). Therefore, we now focus on the relation $q = \mathcal{F}(p_m - p_r)$, in order to precise the response of the model to a pressure difference $(p_m - p_r)$ imposed by the resonator (p_m being fixed). According to equation (6), this requires to express $p_m - p_j = \mathcal{G}(p_m - p_r)$. By combining equations (3), (5) and (15b), we found that $(p_m - p_j)$ is solution of:

$$\begin{aligned} &(p_m - p_j)^3 - 2z_0 k_s (p_m - p_j)^2 \quad + \quad \dots \\ &+k_s^2(z_0^2 + D)(p_m - p_j) - k_s^2 D (p_m - p_r) \quad = 0 \end{aligned} \tag{18}$$

where $D \triangleq \frac{S_c^2}{\alpha^2 w_r^2 \Psi}$. It is obviously possible to solve numerically equation (18). This will be done in paragraph 5.2. However, it is more interesting to obtain properties of the solution according to the values of the model parameters.

5.1 Analytical results

The results below have been obtained analytically. Details of calculations are omitted here. From a general point of view, an increase of Ψ implies an increase of the threshold pressure above which the model may oscillate. More precisely, three behaviors qualitatively different are possible, depending on the value of Ψ. These behaviors will be highlighted in paragraph 5.2. through numerical simulations:

Type 1: when $0 \leq \Psi < \frac{3S_c^2}{\alpha^2 w_r^2 z_0^2}$,
$(p_m - p_j)$ is an increasing function of $(p_m - p_r)$. The behavior is qualitatively the same as the one of the clarinet model presented in section 3 (which corresponds to the case $\Psi = 0$).

Type 2: when $\frac{3S_c^2}{\alpha^2 w_r^2 z_0^2} \leq \Psi < \frac{4S_c^2}{\alpha^2 w_r^2 z_0^2}$,
$(p_m - p_j)$ is a multivaluate function of $(p_m - p_r)$ on a certain range of $(p_m - p_r)$. Then the behavior of the model becomes potentially hysteretic (the presence of hysteresis had been stressed in the case $S_j/S_{ra} \ll 1$ by Mahu ([18]) besides, using numerical simulation but without giving necessary conditions on Ψ). Moreover, one can show that the reed displacement has two possible discontinuities: by varying progressively $(p_m - p_r)$, the reed can jump between two opened-reed positions. These positions are different at closure and at opening.

Type 3: when $\frac{4S_c^2}{\alpha^2 w_r^2 z_0^2} \leq \Psi$,
Conclusions are similar to those obtained for a behavior of type 2, excepted that, by varying progressively $(p_m - p_r)$, the jump of the reed occurs, either from an opened-reed

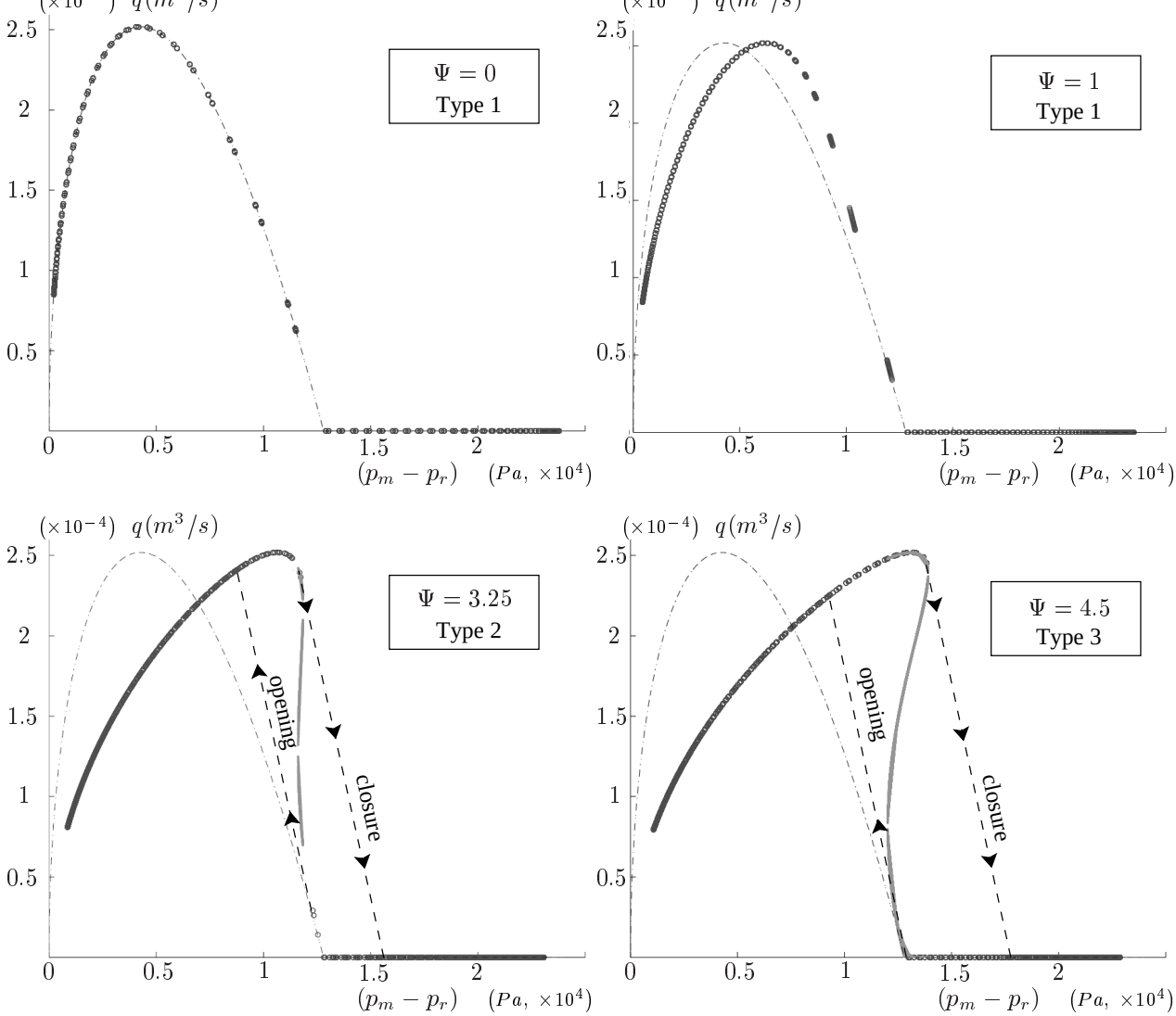

Figure 8: Comparison between analytical expression of the volume flow q if $\Psi = 0$ (equation 6) (dash-doted line) and simulation results (symbol $\circ$) for different values of the discharge losses coefficient Ψ. In the case of multiple solutions, the (clear gray) line represents the set of non chosen solutions.

to a closed-reed position or from a slightly open to a more largely open reed position.

5.2 Numerical simulations

Numerical values of the parameters used in this paragraph are $k_s = 1.6e^{-7}$Pa.m^{-1}, $\alpha = 0.8$, $z_0 = 8e^{-4}$m, $w_r = 7e^{-3}$m, $p_m = 12e^3$Pa, and $l_t = 7.2e^{-1}$m.

As explained in the introduction, at this stage of the study, our aim is to compare results with the well known model of clarinet-like instruments, which explains why conical bores are not considered hereafter. Indeed, a cylindrical resonator is considered (length $l_t = 0.72m$). This allows a straightforward comparison with the simple model of a clarinet, corresponding to the case $\Psi = 0$.

The acoustic response of a cylindrical tube is characterized by its reflexion function (modelled here after some simplifications by a delay and a lowpass filter, even if for sound synthesis purposes the exact reflection function could be preferred). Equations (3), (5), (18) and the acoustic coupling are solved using an iterative scheme in the time domain.

In the case of multiple solutions, a semi-empirical selection rule is applied : the solution chosen belongs to

the same branch of solutions as the solution chosen at the preceding time step, except if this branch has disappeared. Moreover, the solution never belongs to the middle branch because a solution on this branch corresponds neither to a minimum of the potential energy of the reed, nor to a minimum of the potential energy of the flow.

According to analytical results obtained in paragraph 5.1, transitions between regimes noted type 1, type 2 and type 3, occur repectively for $\Psi = 2.89$ and $\Psi = 3.86$. These limit values coincide with those observed on simulation results. On figure 8, four simulation results are presented, corresponding to $\Psi = 0$, $\Psi = 1$, $\Psi = 3.25$ and $\Psi = 4.5$, at 88.2kHz. Each of the four pictures represents the phase space $(q, p_m - p_r)$ for a particular value of Ψ (symbol $\circ$) compared to the case $\Psi = 0$ (dash-doted line). The clear gray line represents the set of non chosen solutions (in the case of multiple solutions).

On figure 9, time-domain solutions of the opening of the double reed are given, whereas on figure 10, time domain solutions of the pressure in the embouchure p_p and the pressure at the beginning at the begining of the resonator p_r can be compared for different values of Ψ. All the results presented in figures 8, 9 and 10 come from the same simulation.

It is worth noting in figures 8 and 9 that when $\Psi = 3.25$ (corresponding to type 2), during the closure phase the reed does not jump between two opened-reed positions before total closure, but directly from an opened position to a closed position. This is not contradictory with the analytical result established in section 5.1 where conclusions are given for a quasi-stationary functioning with infinitesimal variations of $(p_m - p_r)$. This is not always the case when the global model (with a resonator coupled to the flow model) auto-oscillates. Indeed, between two successive samples $(p_m - p_r)$ can vary significantly, as shown by the dashed lines on the bottom part of figure 8 (these lines connect two successive samples at closure and at opening). However a behavior such as the one described in section 5.1 for type 2 has also been observed in simulations for other parameter values.

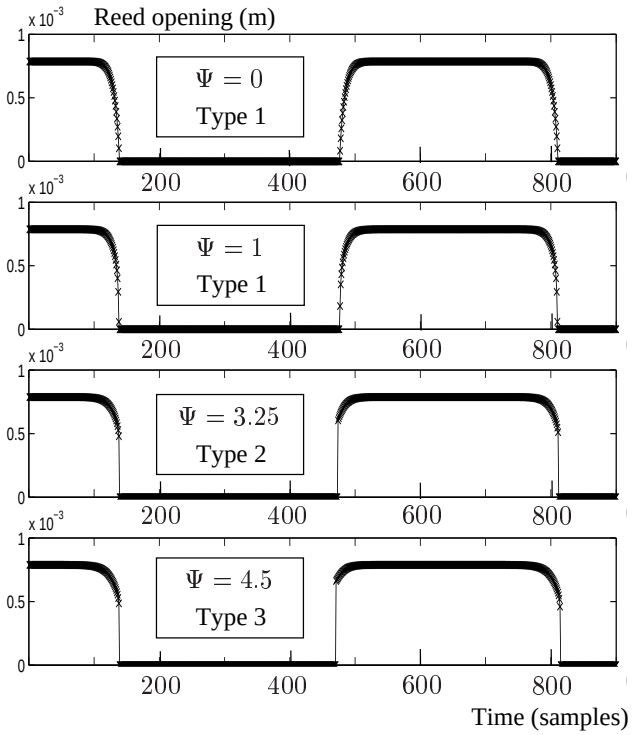

Figure 9: Influence of the coefficient Ψ on the opening of the double reed. Each point is marked by a $\times$ in order to see more easily the modification of the waveshape, as Ψ is increased.

As expected, for the type 3, the reed jumps (when it closes) from a largely opened position to a closed position.

On figure 10, it can be observed that the more Ψ is increased, the more the mean value of p_p is increased. Moreover, for each sample, p_p is greater than p_r. This corresponds to the fact that, for a given pressure difference $(p_m - p_r)$, the pressure difference across the reed $(p_m - p_p)$ (i.e. the pressure difference which tends to move the reed) decreases when Ψ is increased.

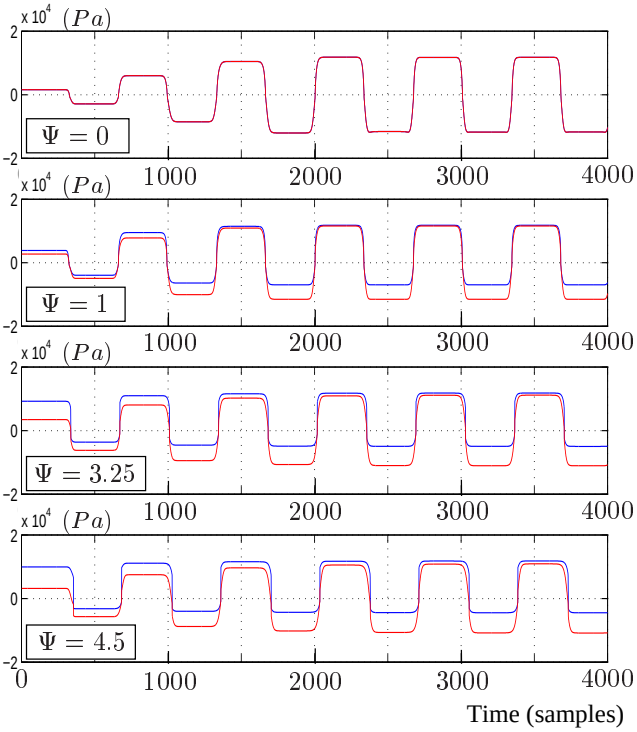

Figure 10: Comparison for different values of Ψ, of the pressure in the embouchure p_p and of the pressure at the begining of the resonator p_r. The more Ψ is increased, the more the mean value of p_p is increased.

6 Discussion

6.1 Estimation of the order of magnitude of Ψ

Let us estimate Ψ according to equation (17). On a Nikuradse diagram (cf. [17] p217) it can be found that for $6e^2 \leq Re_d \leq 1e^4$, $3e^{-2} \leq \zeta_f \leq 1e^{-1}$ for a large range of roughness of the walls. This includes the laminar regime (for which equation (11) can be used to determine ζ_f) and the turbulent regime (assuming a transition around $Re_d \simeq 2000$).

Then according to figure 4, $\Gamma = 0.25$, $S_c = 4.4e^{-6}m^2$, $d = 2.4e^{-3}m$, $L_r = 7.4e^{-2}m$, $w_r = 7e^{-3}m$, $< S_j >_t = \alpha w_r z_0$, with $\alpha = 0.8$ and $z_o = 8e^{-4}m$, $\beta = 7°$. Ψ is found to be close to 2.5. However, this value is highly dependent on many assumptions, in particular the value of α and $< S_j >_t$. Therefore, it is very difficult to give a realistic estimate for Ψ. It is then difficult to determine which type of behavior (among the three) if any, is the most typical of oboe-like instruments. To this end, an experimental determination of Ψ by means of steady flow measurements is being prepared.

6.2 Functioning of the model

An increase of Ψ results in an increase of the pressure difference $(p_m - p_r)$ below which the model cannot oscillate: the pressure difference imposed between the mouth and the instrument is not entirely used to move the fluid (a part is dissipated).

Similarly, the more Ψ is increased, the most difficult it is to obtain regimes where the reed does not beat. Then, evolution in time of the volume flow and of the reed opening becomes close to a square signal. The only control of the volume flow by the reed is performed in this limit case, when the reed is closed.

7 Conclusion

By analysing some essential geometrical differences between embouchures of single reed and double reed instruments, consequences on air flow modeling in the embouchure of each class of instrument have been studied. Within the framework of a quasi-stationary modeling of the double reed, it appears that unlike for the simple reed, the pressure at the inlet of the reed channel and the pressure at the input of the resonator are linked by a nonlinear relationship. This relationship is parameterized by a coefficient Ψ, which encompasses all the differences between the flow model in a simple reed and in a double reed. According to the value of Ψ, three behaviors qualitatively different have been highlighted (analytically and numerically), two of which being potentially hysteretic.

As it has been underlined in this paper, the model has to be considered with care, since several assumptions can

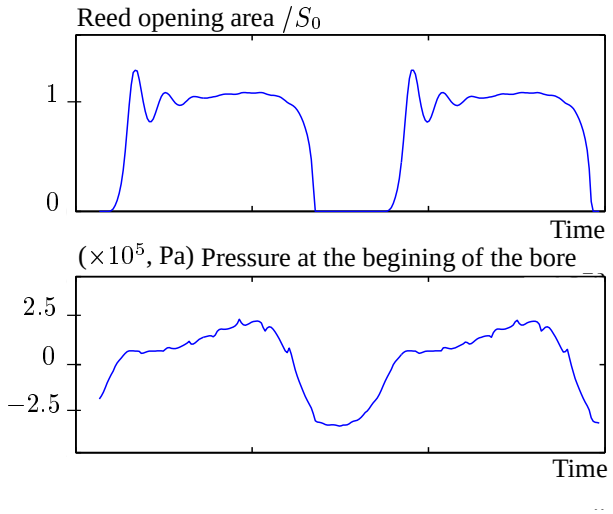

Figure 11: Simulation results of an oboe model : the resonance of the reed and the conical resonator have been taken into account. The upper part is the reed opening area (S_0 is the opening area at rest), whereas the lower part is the pressure at the begining of the bore.

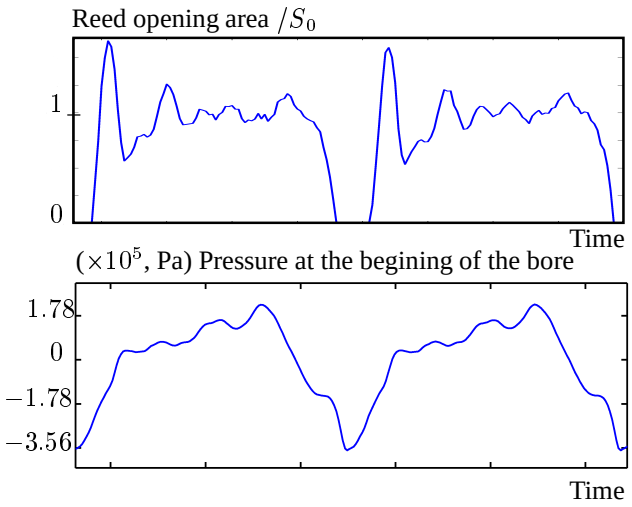

Figure 12: Experimental results obtained with an oboe ([1]): the upper part is the reed opening area (S_0 is the opening area at rest), whereas the lower part is the pressure at the begining of the bore.

be discussed, more particularly those of a bidimensional flow and of a quasi-stationary regime.

At this stage, experimental results are definitely required to decide to which extent the assumptions used to derive equations (15) and (16) are justified. Since the model established relies on a quasi-stationary description of the reed functioning, a first approach could consist in recreating experimentally quasi-stationary conditions. This could be achieved by preventing the reed from oscillating. A measurement of the volume flow and of the pressure at the inlet and at the outlet of the reed could provide results directly comparable with those obtained numerically in figure 8. This has been done successfully in the case of the clarinet by Dalmont and coll. ([19]).

A second approach consists in completing the model in order to make it describe more closely a real instrument and to compare experimental and simulation results. This also allows to take advantage of studies already published (for instance, Gokhshtein [15] and Shimizu [20] on the bassoon). Our most recent work concerns the taking into account of the mass and of the damping of the reed. Moreover a conical resonator has been considered for a direct comparison with an oboe. Preliminary results concern the reed opening area and the pressure at the begining of the bore. Simulation results are presented in figure 11, and have to be compared with experimental results in figure 12 (see [1] for details). For both figures, the upper part is the reed opening area and the lower part is the pressure at the begining of the bore. A qualitative analysis show that numerical and experimental results have obvious ressemblances. Concerning the reed opening, the resonance of the reed just after the reed opening is clearly observable on both figures. The main behavior of the reed is reasonably well reproduced, even if the phase of complete closure lasts longuer in the simulation. Concerning the pressure at the begining of the bore, here again, both signals have similar shapes even if a more detailed and qualitative analysis is obviously needed. Therefore, results presented in figures 11 and 12 are encouraging but are only presented here as an outline of our current research.

References

[1] A. Almeida, C. Vergez, R. Caussé, and X. Rodet. Physical study of double-reed instruments for application to sound-synthesis. In *Proceedings of ISMSA'2002*, Mexico, December 2002. (To appear).

[2] A. Barjau and J. Agulló. Calculation of the Starting Transients of a Double-reed Conical Woodwind. *Acta Acustica*, 69:204–210, 1989.

[3] A. P. J. Wijnands and A. Hirschberg. Effect of a pipe neck downstream of a double reed. In *Proceedings of ISMA95*, pages 149–152, Dourdan, France, 1995.

[4] J. Backus. Small vibration theory of the clarinet. *J. Acoust. Soc. Amer.*, **35**, 305, 1963. and Erratum (61) [1977], 1381.

[5] J. Kergomard. *Mechanics of Musical Instruments (Chap. 6)*, chapter Elementary considerations on reed-instrument oscillations. Springer Verlag, 1995.

[6] A. Hirschberg. *Mechanics of Musical Instruments (Chap. 7)*, chapter Aero-acoustics of wind instruments. Springer Verlag, 1995.

[7] C. J. Nederveen. *Acoustical aspects of woodwind instruments*. Fritz Knuf pub., Amsterdam, 1969.

[8] W. E. Worman. *Self-sustained nonlinear oscillations of medium amplitude in clarinet-like systems*. PhD thesis, Case Western Reserve University, 1971. Ann Arbor University Microfilms (ref. 71-22869).

[9] T. A. Wilson and G. S. Beavers. Operating modes of the clarinet. *J. Acoust. Soc. Amer.*, **56**, 653, 1974.

[10] R. T. Schumacher. Ab initio calculations of the oscillations of a clarinet. *Acustica*, 48:71–85, 1981.

[11] A. Hirschberg, J. Gilbert, A. P. J. Wijnands, and A. M. C. Valkering. Musical aero-acoustics of the clarinet. *Journal de Physique IV*, 4:C5–559:C5–568, Mai 1994. Colloque C5 supplément au Journal de Physique III.

[12] J. Gilbert. *Etude des instruments de musique à anche simple: extension de la méthode d'équilibrage harmonique, rôle de l'inharmonicité des résonances, mesure des grandeurs d'entrée*. PhD thesis, Université du Maine, Novembre 1991.

[13] A. Hirschberg, R. W. A. van de Laar, J. P. Marrou-Maurières, A. P. J. Wijnands, H. J. Dane, S. G. Kruijsswijk, and A. J. M Houtsma. A Quasi-stationary Model of Air Flow in the Reed Channel of Single Reed Woodwind Instruments. *Acta Acustica*, 70:p146–154, 1990.

[14] L. Landau and E. Lifchitz. *Mécanique des fluides*. Number 6 in Collection Physique Théorique. Moscou, Mir edition, 1989. (deuxième édition).

[15] A. Ya. Gokhshtein. Role of airflow modulator in the excitation of sound in wind instruments. *Sov. Phys. Dokl.*, 26(10):954–956, 1981.

[16] S. Candel. *Mécanique des fluides*. Dunod, 1995.

[17] R. Ouziaux and J. Perrier. *Mécanique des fluides appliquée*. 1998. Third edition.

[18] W. E. A. Mahu. Flow induced valve instabilities. Technical report, Technische Universiteit Eindhoven, 1990.

[19] J. P. Dalmont, J. Gilbert, S. Ollivier, and M. Blondet. Nonlinear characteristics of single-reed instruments: quasi-static volume flow and reed opening measurements. *J. Acoust. Soc. Amer.*, 2002. (submitted).

[20] M. Shimizu, T. Naoi, and T. Idogawa. Vibrations of the reed and the air column in the bassoon. *J. Acoust. Soc. Jpn.*, 10(5):269–278, 1989.